J Neurol (2002) 249 : 875–883
DOI 10.1007/s00415-002-0752-y

ORIGINAL COMMUNICATION

M. Cercignani
M. Bozzali
G. Iannucci
G. Comi
M. Filippi

Intra-voxel and inter-voxel coherence in patients with multiple sclerosis assessed using diffusion tensor MRI

Abstract Previous diffusion tensor magnetic resonance imaging (DT-MRI) studies reported mean diffusivity ($\bar{D}$) and fractional anisotropy (FA) changes in lesions and normal-appearing white matter (NAWM) of patients with multiple sclerosis (MS), but neglected the additional information which can be obtained by the analysis of the inter-voxel coherence (C). The present study is based on a large sample of patients with MS and it is aimed at assessing the potential role of C in the quantification of MS-related tissue damage of T2-visible lesions and NAWM.

We obtained dual-echo, T1-weighted and DT-MRI scans from 78 patients with relapsing-remitting (RR), secondary progressive (SP), or primary progressive (PP) MS and from 26 healthy volunteers. We calculated $\bar{D}$, FA and C of T2-hyperintense lesions, T1-isointense lesions, T1-hypointense lesions and several areas of the NAWM.

$\bar{D}$ and FA of the majority of NAWM regions studied from MS patients were different from the corresponding quantities of the white matter from controls. NAWM C from patients was lower than white matter C from controls only for the parietal pericallosal areas. SPMS patients had higher corpus callosum $\bar{D}$ and lower corpus callosum FA and C than patients with either RRMS or PPMS. Average lesion $\bar{D}$ was higher, and average FA and C lower than the corresponding quantities measured in the NAWM. Average T1-hypointense lesion $\bar{D}$ was higher and average FA lower than the corresponding quantities of T1-isointense lesions, whereas average C of these two lesion populations were not different. SPMS had higher average lesion $\bar{D}$ than both PPMS and RRMS patients. NAWM $\bar{D}$ and C of the corpus callosum were moderately correlated with disability.

This study confirms the role of DT-MRI metrics to identify MS lesions with different amounts of tissue damage and to detect diffuse changes in the NAWM. It also shows that measuring C enables us to obtain additional information about tissue damage, which is complementary to that given by the analysis of $\bar{D}$ and FA.

Key words Multiple Sclerosis-Magnetic Resonance Imaging-Diffusion Tensor MRI

Received: 27 July 2001
Received in revised form: 15 January 2002
Accepted: 22 January 2002

M. Cercignani, MPhil · M. Bozzali, MD · G. Iannucci, MD · Massimo Filippi, MD (✉)
Neuroimaging Research Unit
Dept. of Neuroscience
Scientific Institute and University
Ospedale San Raffaele
via Olgettina 60
20132 Milan, Italy
Tel.: +39-02/26 43 30 32
Fax: +39-02/26 43 30 54
E-Mail: filippi.massimo@hsr.it

G. Comi, MD
Clinical Trials Unit
Department of Neuroscience
Scientific Institute and University
Ospedale San Raffaele
Milan, Italy

Introduction

Diffusion-weighted (DW) magnetic resonance imaging (MRI) is a relatively new technique that permits the measurement of water self-diffusivity [23]. Diffusion is the microscopic random translational motion of molecules. In biological tissues, molecular motion can be hindered by the presence of structural barriers and organnelles at a cellular or subcellular level, and can be influenced by the presence of permeable membranes which allow a rapid exchange of water between separate compartments. In the presence of pathological processes that affect the structural characteristics of tissues,

the diffusional motion of water molecules can be altered and result in DW-MRI measurable changes. In tissues with a regular and ordered microstructure, the hindrance of water is not the same in all directions and the diffusion coefficient also depends upon the direction along which it is measured [12, 14]. Under these conditions, diffusion can be characterized by a tensor [5], a 3×3 matrix, where the on-diagonal elements represent the mobility rates in the principal directions of the reference frame, while the off-diagonal elements account for the correlation existing between orthogonal directions. Diffusion tensor (DT) MRI is based on the collection of several DW images with diffusion weightings along non-collinear directions.

In the brain, gray matter and cerebro-spinal fluid (CSF) are isotropic, at least on a voxel scale, while white matter is markedly anisotropic [7, 12]. From the diffusion tensor, it is possible to derive: a) the mean diffusivity ($\bar{D}$), equal to one third of the trace of the tensor, which constitutes a rotationally invariant, directionally averaged diffusion coefficient; b) the fractional anisotropy (FA) [27], which represents one of the most robust indices of anisotropy, and which measures the degree of deviation from isotropic diffusion in every voxel; and c) the principal direction of diffusion, which also provides information about tissue orientation. The degree of anisotropy is highly variable in white matter, ranging from a maximum in regions characterized by a strongly ordered parallel fibers, to much lower values in regions where fibers have incoherent orientations, or where fiber bundles cross. In other words, FA is a measure of the intra-voxel fiber coherence. More recently, an index of inter-voxel coherence (C) has been proposed [26]. C represents the degree of similarity of orientation of adjacent voxels.

Multiple sclerosis (MS) represents an interesting candidate condition for the application of DT-MRI analysis, since the pathological substrates of MS have the potential to alter tissue structure and geometry. Previous studies [11, 13, 15, 18, 19, 37] have found that water diffusivity of MS lesions is increased when compared with that of the normal appearing white matter (NAWM), which, in turn, has greater water diffusivity than the white matter of healthy subjects. In addition, FA has been shown to be significantly modified by MS pathology [11, 19], indicating the presence of decreased tissue organization both in lesions and NAWM. The present study is based on a large sample of patients with the three major phenotypes of the disease and it is aimed at assessing the potential role of C in the quantification of MS-related tissue damage of T2-visible lesions and NAWM.

Patients and methods

Patients

We studied 78 patients with MS (41 women and 37 men). Their mean age was 44.8 years (SD = 11.5), median duration of the disease was 10 years (range = 2–32), and median Expanded Disability Status Scale (EDSS) [21] was 4.5 (range = 0.0–7.5). According to the criteria of Lublin and Reingold [25], 26 patients were classified as having relapsing-remitting (RR), 29 as having secondary progressive (SP) and 23 as having primary progressive (PP) MS. This study was based on a patient sample which was different from those of our previous DT-MRI studies [11, 12, 18, 19]. Twenty-six healthy volunteers (18 women and 8 men; mean age = 45.5 years; SD = 13.8 years), with no previous history of neurological dysfunction and a normal neurological examination, served as controls. Local Ethical Committee approval and written informed consent were obtained from all the subjects before study initiation.

MRI acquisition

All imaging was performed using a 1.5 T scanner (Siemens Vision, Erlangen, Germany). The following sequences were collected from all the individuals during a single MRI session: a) dual-echo turbo spin-echo (TSE) (TR = 3300 ms; first echo TE = 16 ms; second echo TE = 98 ms; echo-train length = 5); b) pulsed-gradient spin-echo echo-planar (EPI) pulse sequence (inter-echo spacing = 0.8 ms, TE = 123 ms), with diffusion gradients applied in eight non collinear directions, chosen to cover three-dimensional space uniformly [20]. The duration and maximum amplitude of the gradients were respectively 25 ms and 21 mT/m^{-1}, giving a maximum b factor in each direction of 1044 s/mm^2. Fat saturation was achieved by using a four radiofrequency pulse binomial pulse train; c) T1-weighted conventional spin-echo (TR = 768 ms, TE = 15 ms).

For the dual-echo and T1-weighted scans, 24 contiguous, 5 mm-thick, axial slices were acquired with a 256×256 matrix and a 250×250 field of view. These slice sets were positioned to run parallel to a line that joins the most inferoanterior and the most inferoposterior parts of the corpus callosum. For the EPI scans, 10 axial slices with 5 mm thickness, 128×128 matrix and 240×240 mm field of view were acquired, with the same orientation of other image sets, with the second last slice positioned to match exactly the central slice of the other sets of images. This brain portion was chosen since the periventricular area is a common site for MS lesions. In addition, these central slices are less affected by distortion induced by B_0 field inhomogeneity.

MRI analysis and post-processing

Hardcopies were revised in a random order by two observers, unaware of the patients' clinical status. Lesions were identified and marked by consensus on the proton density-weighted scans. T2-weighted images were always used to increase confidence in lesion identification. Using T1-weighted scans, lesions identified on the proton density-weighted scans were classified as either T1-isointense or T1-hypointense. Lesions were considered to be T1-hypointense when they had signal intensity between those of the gray matter and CSF [35].

All images were transferred to a workstation (Sun Sparcstation; Sun Microsystem, Mountain View, CA) separate from the scanner for post-processing. EP images were corrected for eddy current-induced geometrical distortion by using an algorithm that assesses the similarity between the diffusion-weighted and the corresponding diffusion-unweighted EP images by maximizing the mutual information [32]. Then, EP images were interpolated to the same matrix size as the dual-echo images, and the b = 0 step of the EP images was coregis-

tered with the long-echo images of the dual-echo scans, using a two-dimensional, third-order warping function, provided by the AIR package [39]. The same transformation parameters were then used to map the EP images on the spatial coordinates of the dual-echo scans. Warping of the original EP images was performed before tensor computation to minimize phase wraparound [26]. Then, assuming a mono-exponential relationship between signal intensity and the product of the b-matrix and diffusion tensor matrix components, the tensor was estimated statistically, using multivariate linear regression [5] according to the following equation:

$$\ln\frac{M}{M_0} = \left(-\sum_{i=1}^{3}\sum_{j=1}^{3} b_{ij}D_{ij}\right),$$

where M is the measured signal intensity, M_0 is the T2-weighted signal intensity, b_{ij} are the elements of the b matrix [4] and D_{ij} are the elements of the diffusion tensor matrix. After diagonalization of the matrix, $\bar{D}$, FA and C were derived for each voxel. C maps were produced as described by Pfefferbaum et al. [26], by calculating the average angle between the eigenvector of the largest eigenvalue of a given voxel and its neighbors, using a 3×3 symmetrical kernel. A typical example of the calculated maps is reported in Fig. 1. Then, a single observer, unaware of MS lesion classification, using the marked hard-copies as a reference, outlined MS lesions on proton density-weighted images displayed on a computer screen using a semi-automated segmentation technique based on local thresholding [30]. Lesion volumes were also measured [30]. The outlined regions of interest (ROIs) were then transferred onto, $\bar{D}$, FA and C maps, and for each patient the average lesion $\bar{D}$, FA and C weighted by lesion area were calculated. $\bar{D}$, FA and C were also measured in different regions of the NAWM. The areas were carefully selected on the dual-echo scans in order to avoid partial volume averaging from the CSF. Rectangular ROIs of variable size (range = 11.4–594.1 mm^2), depending on the anatomical region studied, were placed bilaterally in the white matter of the following areas: the genu and the splenium of the corpus callosum, the posterior limb and the genu of the internal capsule, frontal and parietal pericallosal areas and the centra semiovalia. The genu and the splenium of the corpus callosum were sampled on the three consecutive slices on which they were fully volumed. Frontal and parietal pericallosal ROIs were positioned laterally to the splenium and the genu of the corpus callosum in the same three slices. The posterior limb and the genu of the internal capsule, respectively indexed as the regions bounded by the corner between the head of the caudate nucleus and the pallidum and by the pallidum and the thalamus, were marked on two contiguous slices. The centra semiovalia ROIs were taken from three contiguous slices starting from the most superior slice that included a fully volumed lateral ventricle in at least one hemisphere. Fig. 2 illustrates the location of all the NAWM ROIs. The outlined regions were then transferred onto the DT-MRI derived maps, where areas corresponding to macroscopic lesions had been previously nulled out, and the average NAWM $\bar{D}$, FA and C weighted for the corresponding ROI areas were calculated. The corresponding quantities of the same brain regions were measured from controls.

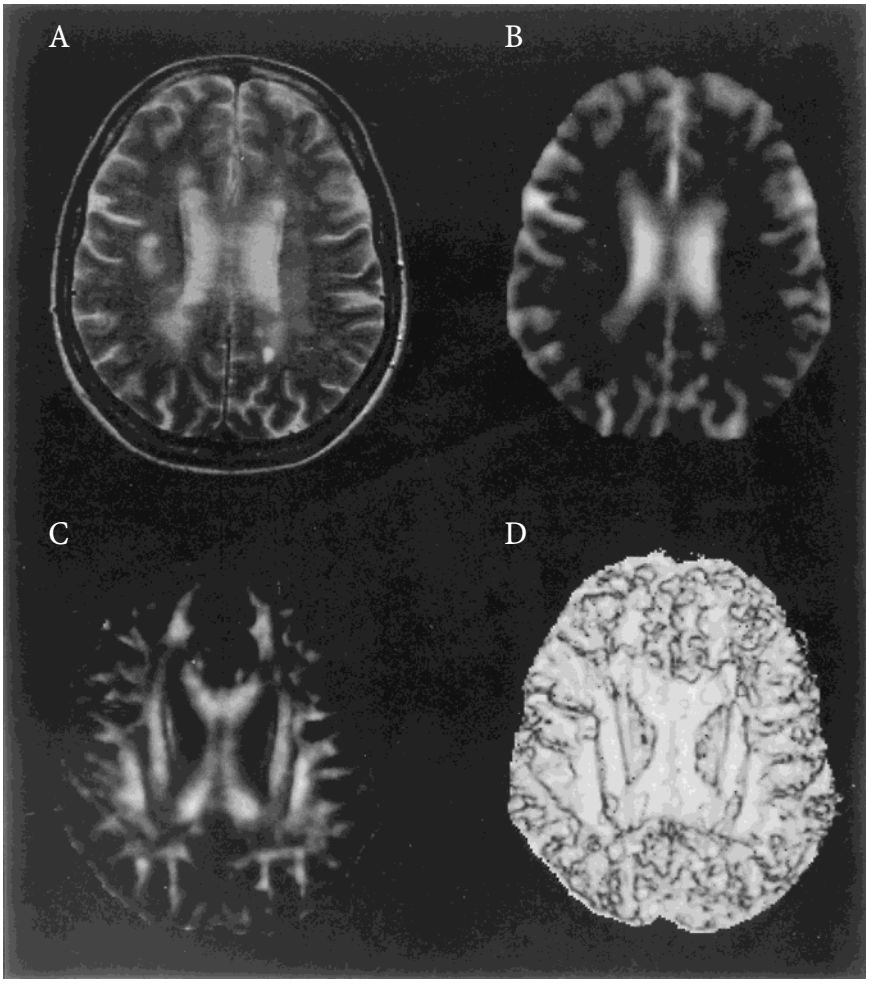

Fig. 1 Axial MR images obtained from a patient with MS. (**A**) T2-weighted image; (**B**) mean diffusivity map; (**C**) fractional anisotropy map; and (**D**) inter-voxel coherence map.

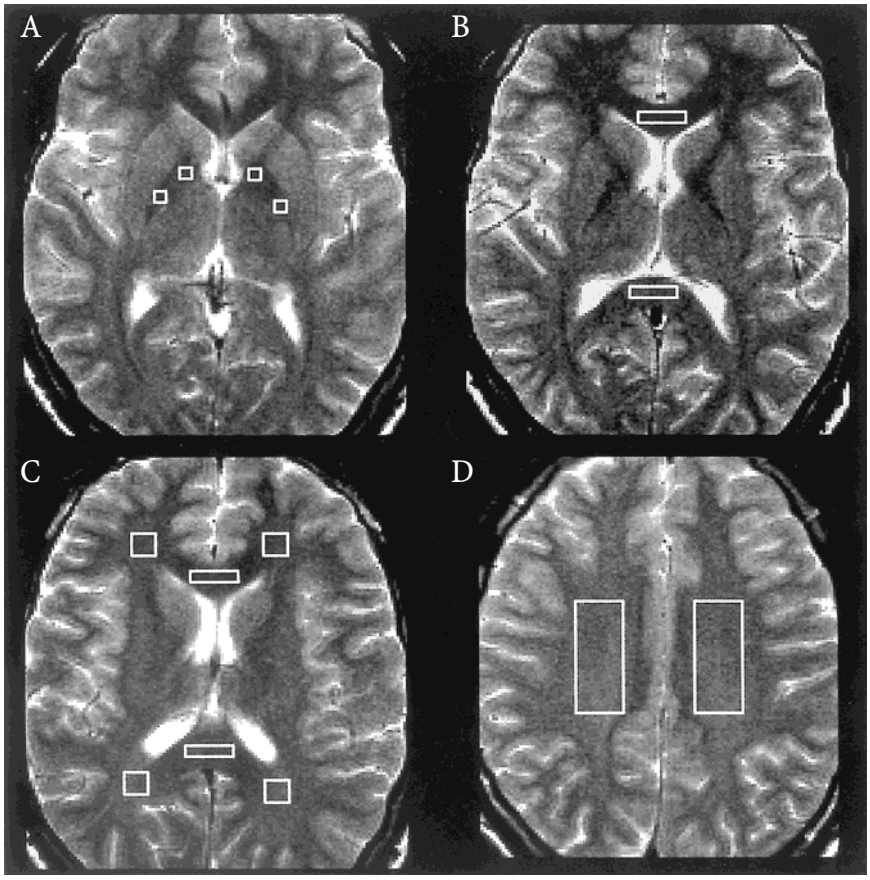

Fig. 2 Location of the regions of interest selected for the analysis of the normal-appearing white matter. (**A**) Genu and posterior limb of the internal capsule; (**B**) genu and splenium of the corpus callosum; (**C**) genu of the corpus callosum with frontal pericallosal areas and splenium of the corpus callosum with parietal pericallosal areas; (**D**) centrum semiovale.

Statistical analysis

A Student's t test for not-paired data was used to compare $\bar{D}$, FA and C values of the NAWM from patients with those of the white matter from controls. The same test was used to compare average values of $\bar{D}$, FA and C, weighted by lesion area, of T1-isointense versus T1-hypointense lesions. A Student's t test for paired data was used to compare the average NAWM $\bar{D}$, FA and C values weighted by ROI area and the corresponding average lesion $\bar{D}$, FA and C weighted by lesion area. A one-way ANOVA was used to assess differences of the three quantities among the three MS phenotypes in the NAWM and in lesions. *Post hoc* analysis was performed using a Student's t test for unpaired samples. To correct for the multiple comparisons and to minimize the risk of type II errors, p values ≤ 0.01 were considered significant, whereas p values between 0.01 and 0.05 were considered trends. Correlations were assessed using the Spearman Rank Correlation Coefficient.

Results

Conventional MRI

No abnormalities were seen on any of the conventional MRI scans obtained from controls. In MS patients, the median T2 lesion volume was 16.8 ml (range: 0.4–106.9 ml) and the median T1-hypointense lesion volume was 2.9 ml (range: 0.0–22.6 ml).

$\bar{D}$, FA and C from the NAWM

Average $\bar{D}$, FA and C values of the NAWM regions studied are reported in Tables 1, 2 and 3, respectively. $\bar{D}$ and FA of the NAWM from MS patients were significantly different or showed a significance trend compared with the corresponding quantities of the white matter from controls in all the regions studied, except for the genu and the posterior limb of the internal capsule. NAWM C from patients was significantly lower than white matter

Table 1 Average (SD) mean diffusivity ($\bar{D}$) of different white matter areas from controls and patients with MS

Anatomical location	Controls	Patients	p
Genu of the corpus callosum	0.89 (0.06)	0.97 (0.09)	0.001
Splenium of the corpus callosum	0.87 (0.08)	0.92 (0.13)	0.01
Genu of the internal capsule	0.83 (0.05)	0.83 (0.06)	n. s.
Posterior limb of the internal capsule	0.76 (0.05)	0.75 (0.05)	n. s.
Frontal pericallosal	0.83 (0.06)	0.87 (0.06)	0.003
Parietal pericallosal	0.87 (0.07)	0.91 (0.09)	0.04
Centrum semiovalis	0.77 (0.05)	0.84 (0.07)	< 0.001
All NAWM areas	0.88 (0.07)	0.80 (0.05)	< 0.001

$\bar{D}$ is expressed in units of $mm^2/s \times 10^{-3}$; *n. s.* not significant; *NAWM* normal-appearing white matter. See text for statistical analysis and further details

Table 2 Average (SD) fractional anisotropy (FA) of different white matter areas from controls and patients with MS

Anatomical location	Controls	Patients	p
Genu of the corpus callosum	0.38 (0.09)	0.47 (0.12)	< 0.001
Splenium of the corpus callosum	0.59 (0.12)	0.67 (0.11)	0.004
Genu of the internal capsule	0.31 (0.08)	0.31 (0.06)	n. s.
Posterior limb of the internal capsule	0.56 (0.06)	0.57 (0.09)	n. s.
Frontal pericallosal	0.26 (0.05)	0.31 (0.06)	< 0.001
Parietal pericallosal	0.32 (0.10)	0.44 (0.12)	< 0.001
Centrum semiovalis	0.26 (0.03)	0.29 (0.03)	< 0.001
All NAWM areas	0.28 (0.03)	0.32 (0.03)	< 0.001

NAWM normal-appearing white matter; *n. s.* not significant. See text for statistical analysis and further details

Table 3 Average (SD) inter-voxel coherence (C) of different white matter areas from controls and patients with MS

Anatomical location	Controls	Patients	p
Genu of the corpus callosum	0.86 (0.04)	0.88 (0.04)	0.05
Splenium of the corpus callosum	0.89 (0.03)	0.91 (0.03)	n. s.
Genu of the internal capsule	0.88 (0.06)	0.91 (0.03)	n. s.
Posterior limb of the internal capsule	0.88 (0.03)	0.88 (0.05)	n. s.
Frontal pericallosal	0.82 (0.04)	0.83 (0.04)	n. s.
Parietal pericallosal	0.81 (0.05)	0.84 (0.04)	0.01
Centrum semiovalis	0.84 (0.02)	0.84 (0.01)	n. s.
All NAWM areas	0.84 (0.07)	0.84 (0.01)	n. s.

NAWM normal-appearing white matter; *n. s.* not significant. See text for statistical analysis and further details

C from controls only for the parietal pericallosal areas, while a significance trend was found for the genu of the corpus callosum. We compared $\bar{D}$, FA and C values from the NAWM also across the three MS phenotypes (Table 4), and found that SPMS patients had significantly reduced average NAWM FA when compared with those with PPMS. A significance trend was also found for average NAWM C. No significant differences were found between PPMS and RRMS and between SPMS and RRMS patients. When considering the corpus callosum in isolation, SPMS patients had higher $\bar{D}$ and lower FA and C than patients with PPMS (Table 4). Corpus callosum $\bar{D}$ of patients with SPMS was also higher than corpus callosum $\bar{D}$ of patients with RRMS. In MS patients, there were moderate correlations between the three quantities derived from NAWM: average $\bar{D}$ vs average FA: $r = -0.43$, $p < 0.001$; average $\bar{D}$ vs average C: $r = -0.33$, $p = 0.004$; average FA vs average C: $r = 0.58$, $p < 0.001$.

$\bar{D}$, FA and C characteristics of macroscopic MS lesions

In the whole of the MS sample, average lesion $\bar{D}$ was $1.19 \pm 0.19 \times 10^{-3}$ mm^2/s, average FA was 0.22 ± 0.03 and average C was 0.82 ± 0.02. These quantities were all significantly different ($p < 0.001$) from those measured in the NAWM ($\bar{D} = 0.88 \pm 0.07 \times 10^{-3}$ mm^2/s; FA $= 0.28 \pm 0.03$; C $= 0.84 \pm 0.01$). Average T1-hypointense lesion $\bar{D}$ was $1.24 \pm 0.21 \times 10^{-3}$ mm^2/s and average FA was 0.20 ± 0.02. These values were both significantly different ($p < 0.001$) from the corresponding quantities of T1-isointense lesions ($\bar{D} = 1.08 \pm 0.07 \times 10^{-3}$ mm^2/s; FA $= 0.24 \pm 0.03$) (Fig. 3). Average C of T1-hypointense lesions (0.82 ± 0.04) and T1-isointense lesions (0.83 ± 0.02) were not significantly different (Fig. 3). All these results were found also when considering the three MS phenotypes separately (data not shown). In addition, we found that SPMS patients had a significantly higher average lesion $\bar{D}$ than those with PPMS and RRMS (Table 4). In MS lesions, a moderate correlation was found between $\bar{D}$ and FA ($r = -0.39$, $p < 0.001$) and between FA and C ($r = 0.37$, $p = 0.001$). No significant correlation was found between $\bar{D}$ and C.

Table 4 Average (SD) lesion and NAWM mean diffusivity ($\bar{D}$), fractional anisotropy (FA) and inter-voxel coherence (C) from the three phenotypes of patients with MS

	SPMS	PPMS	p*	RRMS	p**
Average T2-visible lesion $\bar{D}$	1.29 (0.17)	1.11 (0.21)	0.002	1.14 (0.12)	0.001
Average T2-visible lesion FA	0.21 (0.03)	0.22 (0.04)	n. s.	0.21 (0.02)	n. s.
Average T2-visible lesion C	0.83 (0.01)	0.82 (0.02)	n. s.	0.82 (0.02)	n. s.
Average NAWM $\bar{D}$	0.90 (0.09)	0.87 (0.06)	n. s.	0.87 (0.07)	n. s.
Average NAWM FA	0.27 (0.03)	0.30 (0.03)	0.004	0.28 (0.03)	n. s.
Average NAWM C	0.84 (0.01)	0.85 (0.01)	0.03	0.84 (0.01)	n. s.
Average corpus callosum $\bar{D}$	0.99 (0.10)	0.91 (0.06)	0.002	0.93 (0.09)	0.01
Average corpus callosum FA	0.45 (0.08)	0.53 (0.08)	< 0.001	0.49 (0.08)	n. s.
Average corpus callosum C	0.87 (0.02)	0.89 (0.03)	0.01	0.88 (0.02)	n. s.

$\bar{D}$ is expressed in units of mm^2/s $\times 10^{-3}$. * p values refer to the comparisons between SPMS and PPMS patients; *n. s.* not significant. ** p values refer to the comparisons between SPMS and RRMS patients; *n. s.* not significant. Average corpus callosum $\bar{D}$, FA and C are the mean values obtained by averaging data from the splenium and the genu of the corpus callosum. See text for statistical analysis and further details.
RRMS relapsing-remitting multiple sclerosis; *SPMS* secondary progressive multiple sclerosis; *PPMS* primary progressive multiple sclerosis.

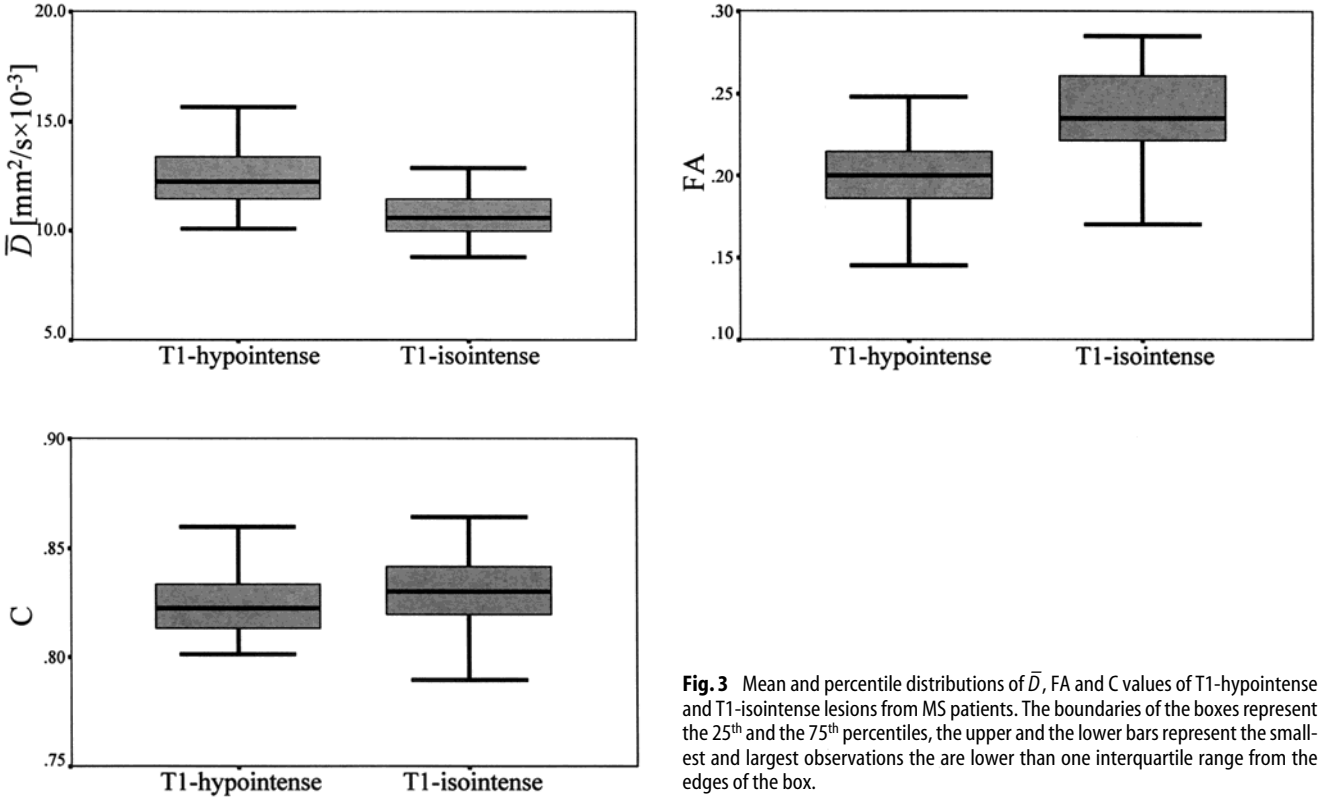

Fig. 3 Mean and percentile distributions of $\bar{D}$, FA and C values of T1-hypointense and T1-isointense lesions from MS patients. The boundaries of the boxes represent the 25th and the 75th percentiles, the upper and the lower bars represent the smallest and largest observations the are lower than one interquartile range from the edges of the box.

Correlations between DT and conventional MRI findings

T2-hyperintense lesion volume was correlated with average lesion FA ($r = -0.40$, $p < 0.001$) and average lesion $\bar{D}$ ($r = 0.46$, $p < 0.001$). T2-hyperintense lesion volume was also correlated with average NAWM $\bar{D}$ ($r = 0.48$, $p < 0.001$), average NAWM FA ($r = -0.70$, $p < 0.001$) and average NAWM C ($r = -0.51$, $p < 0.001$).

Correlations between MRI findings and clinical disability

In the whole of the MS sample, T2 and T1 lesion volumes were not significantly correlated with the EDSS score. No correlation was found between EDSS score and the average lesion $\bar{D}$, FA and C. Similarly, no correlation was found between the EDSS score and the same quantities from the NAWM, when considering all regions together. NAWM $\bar{D}$ and C of the corpus callosum were correlated with EDSS ($r = 0.26$, $p = 0.03$ and $r = -0.28$, $p = 0.01$, respectively). In RRMS patients, NAWM $\bar{D}$ and C of the posterior limb of the internal capsule were correlated with EDSS ($r = 0.38$, $p = 0.05$; and $r = -0.54$, $p = 0.004$, respectively). In SPMS patients, NAWM $\bar{D}$ of the posterior limb of the internal capsule was correlated with EDSS ($r = 0.48$, $p = 0.01$). In PPMS patients, NAWM $\bar{D}$ of the splenium of the corpus callosum was correlated with EDSS ($r = 0.45$, $p = 0.04$).

Discussion

DT-MRI enables us to infer structural properties of biological tissues *in vivo* [6]. As a consequence, it is increasingly been applied to assess tissue damage associated to diseases of the central nervous system [31], including MS [3, 11, 19, 37]. However, previous DT-MRI studies of MS were focussed on measurement of $\bar{D}$ and FA and neglected the additional information which can be conveyed by the analysis of the principal direction of diffusion in every voxel. In white matter, which is a highly ordered tissue, the predominant orientation of diffusion is likely to reflect the axonal fiber orientation. Recently, an index of "inter-voxel coherence", which represents the degree of alignment between neighboring voxels, has been proposed [26]. Using such an approach, regional differences in FA and C in healthy volunteers have been investigated [26], as well as the effect of age and sex on these quantities [33]. Against this background, we measured intra- (FA) and inter-voxel (C) coherence in patients with MS in order to elucidate the relationship between these two DT-MRI quantities in the

presence of a condition with the potential to alter the geometry of brain tissue structure, and to investigate how this new measure might improve our understanding of MS pathophysiology.

The first result of this study is that C values of both lesions and NAWM are only moderately correlated with $\bar{D}$ and FA values of the corresponding tissues. Although longitudinal studies correlating changes of quantities derived from DT-MRI are needed to clarify this issue, this observation indicates that measuring C of different MS tissues might be rewarding in terms of a more accurate quantification of MS structural damage, since it gives information, which is, at least partially, independent from that conveyed by $\bar{D}$ and FA. Because tissue loss alone would both increase $\bar{D}$ and decrease FA and C, other pathological substrates of the disease, such as gliosis or remyelination might account for the limited correlation found between these quantities. Reactive gliosis following tissue injury might, on the one hand, restore barriers restricting water molecular motion (and, as a consequence, lead to a "pseudo-normalization" of $\bar{D}$) and, on the other, since it is a rather structurally disorganized process [22], might also be associated with reduced FA and C values. Thus, the presence of substantial glial proliferation in the MS diseased tissue might lessen the magnitude of the correlation between $\bar{D}$, FA and C. On the contrary, remyelination should result in the restoration of FA and C toward normality, but should also be associated with increased $\bar{D}$ values due to the reduced sizes of the remyelinated fibers [22]. Again, this would lessen the magnitude of the correlation between $\bar{D}$, FA and C in areas where prominent remyelination has occurred. All the above considerations suggest the potential of serial DT MRI to monitor tissue repair in MS.

Our results confirm that $\bar{D}$ and FA are highly variable in MS lesions and different from those of the NAWM [19, 37]. We also found that C of T2-visible lesions is lower than that of the NAWM. However, while $\bar{D}$ was significantly increased and FA significantly decreased in T1-hypointense compared with T1-isointense lesions, C did not differ significantly between these two lesion populations. This agrees with the results of previous *post-mortem* [8, 9] and *in-vivo* quantitative MRI studies [19, 24] showing that the extent of tissue damage is extremely variable in individual T1-hypointense lesions. Although these lesions correspond to areas where chronic severe tissue disruption has occurred [36], the identification of individual T1-hypointese lesions is based on a binary classification and, as a consequence, T1-hypointense volume measurements do not provide graded information about intrinsic pathology of individual lesions. Admittedly, we did not inject gadolinium and, therefore, we were unable to limit our analysis to chronic T1-hypointensities. Nevertheless, acute T1-hypointense lesions are likely to represent a small minority of the overall lesions studied and likely not to influence our results very much. Also, owing to the high regional variability of DT-MRI quantities [3], comparisons between C and FA values should be always limited to the brain regions from which these quantities have been measured. Clearly, this is not possible when assessing MS lesions, whose location is highly variable. Nevertheless, the large amount of lesions studied should have limited the impact of such variability on the C values we measured for T1-isointense and T1-hypointense lesions.

We also measured $\bar{D}$, FA and C from different regions of the NAWM. Previous *post-mortem* [2, 16], magnetization transfer MRI [17, 34], DW-MRI [10] and DT-MRI [18, 19, 29, 38] studies showed that tissue damage does occur outside T2-visible lesions. The pathological substrates of these changes are still unclear. The increased $\bar{D}$ of the NAWM from MS patients compared with the $\bar{D}$ of the white matter of controls in most of the regions studied is consistent with a widespread loss of structural barriers to water molecular motion. Consistently, also FA was found to be significantly decreased in most of the NAWM regions studied. Although the reason for diffusion being anisotropic in the normal mature white matter is still unclear, the most plausible explanation is that it is the result of the concurrent presence of several oriented structures, such as the myelin sheaths, the axons, and the filamentous cytoskeleton [7]. Thus, reduced FA values of several regions of the NAWM of MS patients suggests the presence of a diffuse loss of myelin and axons. Since C is a measure of inter-voxel coherence, reduced C values might be thought as an index of more marked tissue disorganization than the presence of FA changes alone. Consistently with these observations, we found abnormal C values only in the parietal pericallosal area and in the genu of the corpus callosum. Interestingly, the parietal pericallosal area is a typical location of MS lesions [22], and the genu of the corpus callosum is mainly composed of large bundles of highly-oriented myelinated fibers [1].

$\bar{D}$, FA and C were moderately correlated with both T2-hyperintense and T1-hypointense lesion volumes. This provides support for the concept that the diffuse damage of the NAWM is not merely the result of Wallerian degeneration of axons traversing larger lesions. DT-MRI derived measures were only weakly correlated with clinical disability. Nevertheless, DT-MRI quantities measured in the corpus callosum or in the internal capsule were correlated moderately with the EDSS scores of individual patients groups. This fits well with the frequent demonstration of cognitive impairment and locomotor disability in patients with MS. We focused our analysis on these brain structures because of their size which is suitable for ROI analysis, and because they have homogeneous fiber geometries which make DT-MRI measurements more robust than those obtained from other areas. In addition, the corpus callosum and the in-

ternal capsule are sites typically involved by the MS pathological process [22].

In conclusion, this study confirms the role of DT-MRI metrics to identify MS lesions with different amounts of tissue damage and to detect diffuse changes in the NAWM. It also shows that measuring C enables us to obtain additional information about tissue damage, which is complementary to that given by the analysis of $\bar{D}$ and FA. Longitudinal multiparametric MR studies are needed to establish the role of DT-MRI in the monitoring of patients with MS and the relative contribution of DT-MRI metrics in the understanding of disease pathophysiology in the context of the many available quantitative MR techniques [40].

References

1. Aboitz F, Sckeibel A, Fisher R, Zaidel E (1992) Fiber composition of the human corpus callosum. Brain Res 598: 143–153
2. Allen I, McKeown S (1979) A histological, histochemical and biochemical study of the macroscopically normal white matter in multiple sclerosis. J Neurol Sci 41:81–91
3. Bammer R, Augustin M, Strasser-Fuchs S, Seifert T, Kapeller P, Stollberger R, Ebner F, Hartung HP, Fazekas F (2000) Magnetic resonance diffusion tensor imaging for characterizing diffuse and focal white matter abnormalities in multiple sclerosis. Magn Reson Med 44:583–591
4. Basser PJ, Mattiello J, LeBihan D (1994) MR diffusion tensor spectroscopy and imaging. Biophys J 66:259–267
5. Basser PJ, Mattiello J, Le Bihan D (1994) Estimation of the effective self-diffusion tensor from the NMR spin-echo. J Magn Reson B 103:247–254
6. Basser PJ, Pierpaoli C (1996) Microstructural and physiological features of tissue elucidated by quantitative diffusion-tensor MRI. J Magn Reson B 11:209–219
7. Beaulieu C, Allen PS (1994) Determinants of anisotropic water diffusion in nerves. Magn Reson Med 31:394–400
8. Bitsch A, Kuhlmann T, Stadelmann C, Lassmann H, Lucchinetti C, Bruck W (2001) A longitudinal MRI study of histopathologically defined hypointense multiple sclerosis lesions. Ann Neurol 49:793–796
9. Brück W, Bitsch A, Kolenda H, Brück Y, Stiefel M, Lassmann H (1997) Inflammatory central nervous system demyelination: correlation of magnetic resonance imaging findings with lesion pathology. Ann Neurol 42:783–793
10. Cercignani M, Iannucci G, Rocca MA, Comi G, Horsfield MA, Filippi M (2000) Pathologic damage in MS assessed by diffusion-weighted and magnetization transfer MRI. Neurology 54:1139–1144
11. Cercignani M, Inglese M, Pagani E, Comi G, Filippi M (2001) Mean diffusivity and fractional anisotropy histograms in patients with multiple sclerosis. AJNR Am J Neuroradiol 22: 952–958
12. Chenevert TL, Brunberg JA, Pipe JG (1990) Anisotropic diffusion in human white matter: demonstration with MR techniques in vivo. Radiology 177: 401–405
13. Christiansen P, Gideon P, Thomsen C, Stubgaard M, Henriksen O, Larsson HBW (1993) Increased water self-diffusion in chronic plaques and in apparently normal white matter in patients with multiple sclerosis. Acta Neurol Scand 87:195–199
14. Cleveland GG, Chang DC, Hazlewood CF, Rorschach HE (1976) Nuclear magnetic resonance measurement of skeletal muscle. Biophys J 16:1043–1053
15. Droogan AG, Clark CA, Werring DJ, Barker GJ, McDonald WI, Miller DH (1999) Comparison of multiple sclerosis clinical subgroups using navigated spin echo diffusion-weighted imaging. Magn Reson Imaging 17:653–661
16. Evangelou N, Konz D, Esiri MM, Smith S, Palace J, Matthews PM (2000) Regional axonal loss in the corpus callosum correlates with cerebral white matter lesion volume and distribution in multiple sclerosis. Brain 123: 1845–1849
17. Filippi M, Campi A, Dousset V, Baratti C, Martinelli V, Canal N, Scotti G, Comi G (1995) A magnetization transfer imaging study of normal-appearing white matter in multiple sclerosis. Neurology 45:478–482
18. Filippi M, Iannucci G, Cercignani M, Rocca MA, Pratesi A, Comi G (2000) A quantitative study of water diffusion in multiple sclerosis lesions and normal-appearing white matter using echo-planar imaging. Arch Neurol 57: 1017–1021
19. Filippi M, Cercignani M, Inglese M, Horsfield MA, Comi G (2001) Diffusion tensor magnetic resonance imaging in multiple sclerosis. Neurology 56:304–311
20. Jones DK, Horsfield MA, Simmons A (1999) Optimal strategies for measuring diffusion in anisotropic systems by magnetic resonance imaging. Magn Reson Med 42:515–525
21. Kurtzke JF (1983) Rating neurological impairment in multiple sclerosis: an expanded disability status scale (EDSS). Neurology 33:1444–1452
22. Lassman H (1998) Pathology of multiple sclerosis. In: Compston A, Lassman H, McDonald I, Matthews B, Wekerle H (eds) McAlpine's Multiple Sclerosis (3rd edition). Churchill Livingstone, London, pp 323–358
23. Le Bihan D, Turner R, Pekar J, Moonen CTW (1991) Diffusion and perfusion imaging by gradient sensitization: design, strategy and significance. J Magn Reson Imaging 1:7–8
24. Li BSY, Moriarty DM, Regal J, Mannon LJ, Grossman RI, Gonen O (2001) In vivo 3D 1H MRS of T1-hypointense lesions in relapring-remitting multiple sclerosis (abstract). Proc Intl Soc Mag Reson Med 9:470
25. Lublin FD, Reingold SC for the National Multiple Sclerosis Society (USA) Advisory Committee on Clinical Trials of New Agents in Multiple Sclerosis (1996) Defining the clinical course of multiple sclerosis: results of an international survey. Neurology 46:907–911
26. Pfefferbaum A, Sullivan EV, Hedehus M, Lim KO, Adalsteinsson E, Moseley M (2000) Age related decline in brain white matter anisotropy measured by spatially corrected echo-planar diffusion tensor imaging. Magn Reson Med 44:259–268
27. Pierpaoli C, Basser PJ (1996) Towards a quantitative assessment of diffusion anisotropy. Magn Reson Med 36: 893–906
28. Pierpaoli C, Jezzard P, Basser PJ, Blarnett A, Di Chiro G (1996) Diffusion tensor MR imaging of the human brain. Radiology 201:637–648
29. Rocca MA, Cercignani M, Iannucci G, Comi G, Filippi M (2000) Weekly diffusion-weighted imaging study of NAWM in MS. Neurology 55:882–884
30. Rovaris M, Filippi M, Calori G, Rodegher M, Campi A, Colombo B, Comi G (1997) Intra-observer reproducibility in measuring new putative MR markers of demyelination and axonal loss in multiple sclerosis: a comparison with conventional T2-weighted images. J Neurol 244:266–270
31. Schaefer PW (2001) Applications of DWI in clinical neurology. J Neurol Sci 186 (Suppl. 1):S25–35

32. Studholme C, Hill DLG, Hawkes DJ (1996) Automated three-dimensional registration of magnetic resonance and positron emission tomography brain images by multiresolution optimization of voxel similarity measures. Med Phys 24:25–35
33. Sullivan EV, Adalsteisson E, Hedehus M, Ju C, Moseley M, Lim KO, Pfefferbaum A (2001) Equivalent disruption of regional white matter microstructure in ageing healthy men and women. Neuroreport 12:99–104
34. Tortorella C, Viti B, Bozzali M, Sormani MP, Rizzo G, Gilardi MC, Comi G, Filippi M (2000) A magnetization transfer histogram study of normal appearing brain tissue in multiple sclerosis. Neurology 54:186–193
35. van Waesberghe JH, van Walderveen MAA, Castelijns JA, Scheltens P, Lycklama á Nijeholt GJ, Polman C, Barkhof F (1998) Patterns of lesion development in multiple sclerosis: longitudinal observations with T1-weighted spin-echo and magnetization transfer MR. AJNR, Am J Neurariol 19:675–683
36. van Walderveen MA, Kamphorst W, Scheltens P, van Waesberghe JH, Ravid R, Valk J, Polman C, Barkhof F (1998) Histopathologic correlate of hypointense lesions on T1-weighted spin-echo MRI in multiple sclerosis. Neurology 50:1282–1288
37. Werring DJ, Clark CA, Barker GJ, Thompson AJ, Miller DH (1999) Diffusion tensor imaging of lesions and normal-appearing white matter in multiple sclerosis. Neurology 52: 1626–1632
38. Werring DJ, Brassat D, Droogan AG, Clark CA, Symms MR, Barker GJ, MacManus DG, Thompson AJ, Miller DH (2000) The pathogensis of lesions and normal-appearing white matter changes in multiple sclerosis. Brain 123:1667–1676
39. Woods R, Grafton S, Holwes C, Cherry S, Mazziotta J (1998) Automated image registration I. General methods and intrasubject intramodality validation. J Comput Assist Tomogr 22:139–152
40. Filippi M, Grossman RI (2002) MRI techniques to monitor MS evolution: the present and the future. Neurology in press